ISSN 1392-1207. MECHANIKA. Vol. 30, No. 2, 2024: 168–176

Vibration Characteristics Analysis of Twin-Screw Compressor Shell Based on the Fluid-Solid Coupling Method

Yayin HE*, Wei ZHANG, Xuyang HE***, Kai WANG****, Junli WANG*****, Yongqiang ZHAO******

**Shaanxi University of Technology, Hanzhong 723000, China, E-mail: heyayin@21cn.com (Corresponding author)*
***Shaanxi University of Technology, Hanzhong 723000, China, E-mail: 1433810649@qq.com*
****Shaanxi University of Technology, Hanzhong 723000, China, E-mail: 2511606454@qq.com*
*****Shaanxi University of Technology, Hanzhong 723000, China, E-mail: 852405182@qq.com*
******Shaanxi University of Technology, Hanzhong 723000, China, E-mail: wjl503@126.com*
*******Shaanxi University of Technology, Hanzhong 723000, China, E-mail: zyq0620@126.com*

https://doi.org/10.5755/j02.mech.33175

1. Introduction

The twin-screw compressor is a widely used rotary fluid machine. The working process is realized by the rotating meshing action of the negative and positive rotors, including the three processes of compressor suction, compression and discharge. During operation, the compressor shell is subjected to excitation forces consisting of two parts: one part is the force generated by the surrounding fluid acting directly on the shell, that is, the surface flow field force; the other part is the restrained reaction force of the rotor transferred to the shell through the bearing. Under the action of these excitation forces, the compressor shell will produce vibration, and as the main bearing parts of the compressor vibration, the shell vibration characteristics analysis is the basis of compressor vibration reduction and noise reduction.

Over the years, many scholars at home and abroad have conducted relevant studies on compressor vibration. Xue Houqiang [1] et al. established a finite element dynamics model and an acoustic boundary element model to study the structural radiation noise characteristics of a marine air compressor structure, and solved the vibration response of the air compressor structure by using the dynamic excitation generated by the crankshaft rotation as the vibration excitation; Huang [2] et al. studied the vibration of the reciprocating compressor mainframe, using a combination of transient response analysis and experimental tests, and the results showed that the maximum vibration deformation of the mainframe occurred at the end of the four cylinders, and the maximum stress occurred at the connection between the primary inlet buffer tank and the four cylinders. Leila [3] et al. evaluated the vibration signals of twin-screw refrigeration compressors using CFD software applying flow field pressure loads to a rotor-bearing system based on multi-body dynamics; Li Chao [4] et al. analyzed the variation law of the crank force and angular acceleration of the drive bearing of the scroll compressor under different clearances, using the multi-body dynamics theory，and analyzed the transient dynamic response of the rotor under different angular acceleration excitation using the finite element method; Jiang Shijie [5] et al. conducted a dynamic experimental study of centrifugal compressor impeller and simulated the impeller based on the vibration signals collected; For the reciprocating compressor pipeline vibration problem, Li Shuxun [6] et al. performed pressure pulsation calculation and fluid-solid coupling modal analysis on the pipeline, and the results showed that the vibration was caused by the fluid pressure pulsation frequency and the pipeline mechanical inherent frequency falling within the resonance region of the compressor excitation frequency. Wang [7] et al. established a dynamic simulation model of scroll compressor and analyzed its time domain characteristics and frequency domain characteristics under bearing excitation and support excitation, meanwhile, the transient dynamic response of scroll compressor under the action of excitation source was analyzed; Liu Libo [8] et al. established a scroll compressor vibration test experimental system and studied the vibration contribution of the main components of scroll compressor to the whole machine, the results showed that the rotor system dynamic balance is the main source of vibration triggering the whole machine, and the vibration contribution ratio of the main bearing position of the drive shaft is the largest. Xu [9] et al. simulated the internal flow field, structural vibration and external noise of a centrifugal compressor using finite element techniques, and studied the vibration and noise caused by unsteady flow inside the centrifugal compressor; Yang Fan [10] et al. established a fluid-solid coupling model for air conditioning pipeline to obtain the surface pressure on the inner wall of the pipeline under pulsating excitation, meanwhile, the harmonic response analysis of the pipeline system was carried out with compressor vibration and pressure on the inner surface of the pipe as the excitation source, which finally showed that fluid pressure fluctuation has an important influence on the dynamics analysis of the pipeline system.

It can be seen that the above-mentioned scholars have studied the impeller vibration, bearing excitation and piping system vibration of scroll compressors and centrifugal compressors, but there are fewer studies on the shell vibration of screw compressors under the excitation of flow field force and rotor binding force reaction. In this paper, the flow-solid coupling method is used to study the vibration response of the shell under the excitation force by using the flow field pressure and the rotor binding force reaction as the shell vibration excitation source.

2. Vibration characteristic calculation method

This article uses the Fluent and Transient Structural modules in the Workbench platform. The internal flow field of twin-screw compressor is simulated by Fluent modules. Based on the fluid-solid coupling calculation method, the

convergent pressure field is loaded on the negative and positive rotors by numerical interpolation technology, and then the constraint force of the rotors is analyzed by Transient Structural modules. Finally, the dynamic response of the shell is solved by loading the pressure field and the rotor constraint force on the compressor shell. The specific process is shown in Fig. 1.

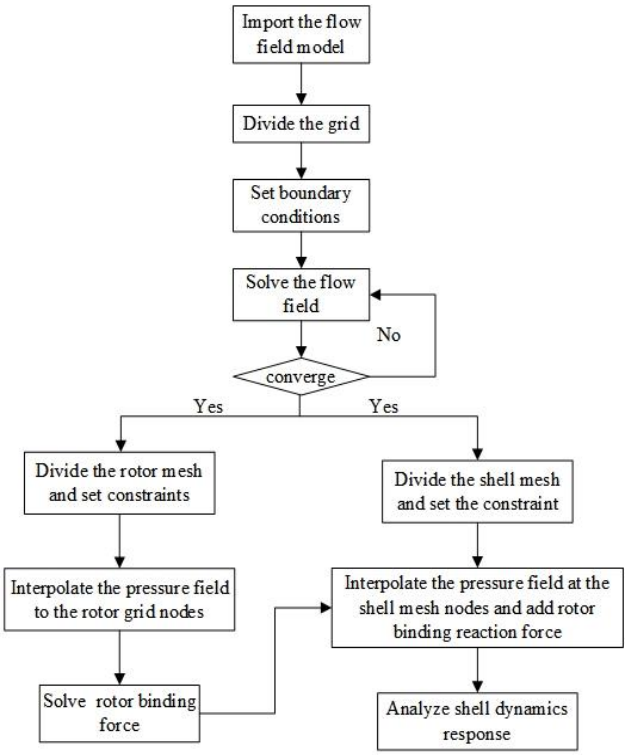

Fig. 1 Flow chart of shell dynamic response analysis

2.1. Aerodynamic force solution method

The flow field simulation of the compressor is performed to solve the pressure field generated during the rotor operation in order to consider the rotor surface loading. The paper focuses on the shell vibration response under the flow field pressure and rotor binding force reaction excitation, and neglect the effect of flow field temperature on the shell, its mass and momentum conservation equations are as follows [11]:

$$\left.\begin{aligned} \frac{\partial \rho}{\partial t}+\nabla(\rho v)=0 \\ \frac{D(\rho v)}{Dt}=\rho F-\nabla p+u\Delta v \end{aligned}\right\}, \quad (1)$$

where: ρ is the density of the fluid, t is the time, v is the velocity tensor, F is the mass force acting on the fluid, p is the fluid pressure and u is the dynamic viscosity of the fluid.

2.2. Solving method of structural motion equation

Through transient dynamics calculation, the response results of displacement and stress of the structure with time under transient load excitation are obtained. The finite element model of the compressor shell is considered as an elastic system with finite degrees of freedom. According to the mechanical theory, the equations of motion of the shell can be formulated as follows [12-13]:

$$\{M\}\{\ddot{\delta}\}+\{C\}\{\dot{\delta}\}+\{K\}\{\delta\}=\{R(t)\}, \quad (2)$$

where, M is the total mass matrix of the compressor shell, δ is the shell displacement matrix, C is the damping matrix of the compressor shell, K is the total stiffness matrix of the compressor shell, $R(t)$ is the load matrix of the compressor shell, and the compressor shell load includes flow field pressure and rotor constraint force.

3. Twin-screw compressor shell excitation analysis

The LGY-03 twin-screw compressor shell is the object of study in this paper. Before analyzing the shell vibration characteristics of a twin-screw compressor, the shell vibration excitation source needs to be solved.

Firstly, the compressor flow field model was established to analyze the compressor flow field and solve the compressor internal flow field pressure distribution; secondly, the flow field force was applied to the negative and positive rotor to solve the rotor binding force by dynamics analysis. The specific parameters of the rotors are shown in Table 1, and the compressor flow field model and rotor model are shown in Fig. 2.

Table 1

Negative and positive rotor parameters

Rotor type	Rotation direction	Number of teeth	Outer circle, mm	Root Circle, mm	Lead, mm	Axial length, mm
Positive rotor	Right rotation	5	115.88	71.211	260	225
Negative rotor	Left rotation	6	92.66	47.998	312	225

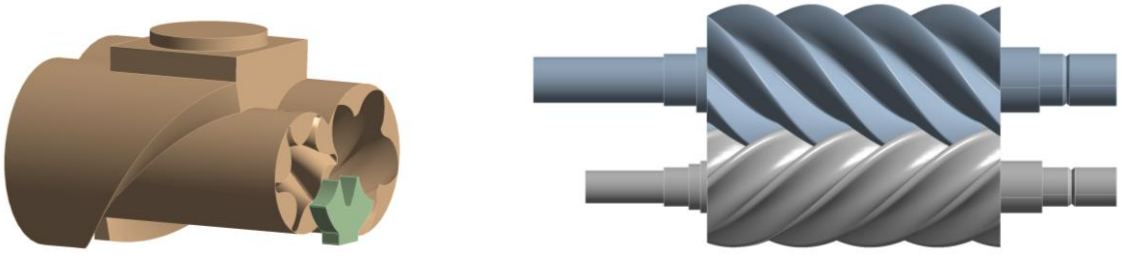

a b

Fig. 2 Flow field and rotor model: a – flow field model; b – rotor model

3.1. Flow field analysis

Due to the existence of complex spiral surfaces in the flow field model, tetrahedral cells are used to mesh it, and finally the mesh quality is checked by cell mass and orthogonal mass to check whether it meets the requirements. The flow field meshing and boundary condition naming are shown in Fig. 3. The number of meshes is 1398886, and the average values of cell mass and orthogonal mass are 0.82814 and 0.76271 respectively, which meet the requirements of solution accuracy.

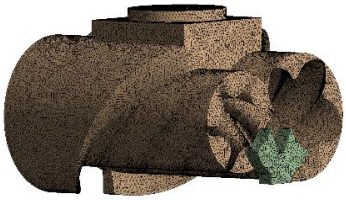

a

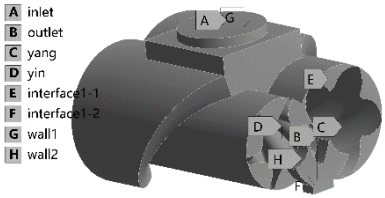

b

Fig. 3 Grid division and boundary naming: a – grid division b – boundary naming

In the flow field analysis of the compressor, the gravitational acceleration size is set to 9.81 m/s^2 and the turbulence model is selected as the standard model $k-\varepsilon$. Set the compressor suction port as the pressure inlet and the suction port pressure size is 0.1 MPa; Set the compressor exhaust port as the pressure outlet, and the size of the exhaust port pressure is 0.8 MPa. Set the negative rotor and positive rotor wall as the rotating wall, the motion is absolute velocity motion, where the size of the wall speed of the positive rotor is 418.9 rad/s and the size of the wall speed of the negative rotor is 355 rad/s, set the outer wall surface of the flow field as a static wall surface, select the pressure-velocity solver. According to the speed, the rotation time of the positive rotor is 0.015 s, set the time step to 0.00015 s and set the number of time steps to 100.The distribution of the pressure field under the above conditions is calculated and solved as shown in Fig. 4.

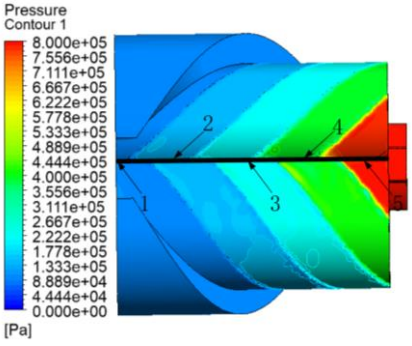

Fig. 4 Flow field pressure distribution

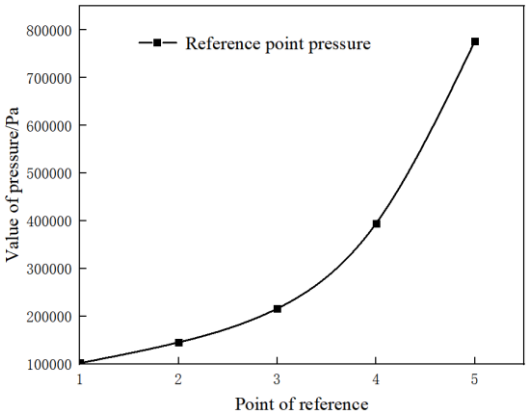

Fig. 5 Reference point pressure curve

It can be seen from Fig. 4, the location of the maximum compressor flow field pressure is at the exhaust port, and the flow field pressure at the suction port is relatively small. In order to analyze the pressure, change trend between the suction port and the exhaust port more intuitively, the flow field is divided into five regions according to the color of the flow field pressure gradient, and five reference points are set equidistantly on the junction line of the negative and positive rotor walls, as shown in Fig. 4. The pressure variation curve at the reference point is shown in Fig. 5. As shown in Fig. 5, the pressure in the flow field gradually increases from the suction port to the exhaust port, but the trend is nonlinear, and the pressure jumps more and more as it gets closer to the exhaust port.

3.2. Rotor binding analysis

During the operation of the twin-screw compressor, the flow field force on the rotor surface and the binding force on the rotor rotation are finally acted on the compressor housing through the bearing, that is, the rotor binding reaction force. The pressure field obtained from the flow field analysis is applied to the surface of negative rotor and positive rotor, the pressure load is shown in Fig. 6.

The rotor of the twin-screw compressor is positioned by means of bearings, where the ball bearings achieve axial positioning and withstand axial force, the roller bearings achieve radial positioning and withstand radial forces. To ensure a constant minimum clearance at the

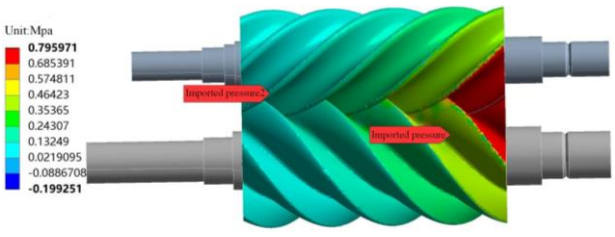

Fig. 6 Pressure load

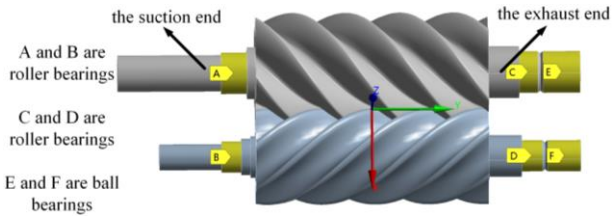

Fig. 7 Bearing mounting position

exhaust end to prevent leakage and avoid end-face wear, the rotor of a twin-screw compressor is generally positioned axially at the exhaust end, leaving a certain axial clearance at the suction end to allow free expansion. The specific location of the bearing installation is shown in Fig. 7. Therefore, the restraint to limit axial movement and retain rotation around the shaft is set at the mounting position of the ball bearing at the exhaust end; and the restraint to retain rotation around the shaft and axial movement and limit the remaining degrees of freedom is set at the mounting position of the roller bearing. According to the positive rotor speed, the solution end time is set to 0.015 s, the rotation angle is 360 degrees, that is, the positive rotor speed is 418.9 rad/s, and the time step is set to 100.Contact was set on the surface of the negative and positive rotor, and the contact type was set

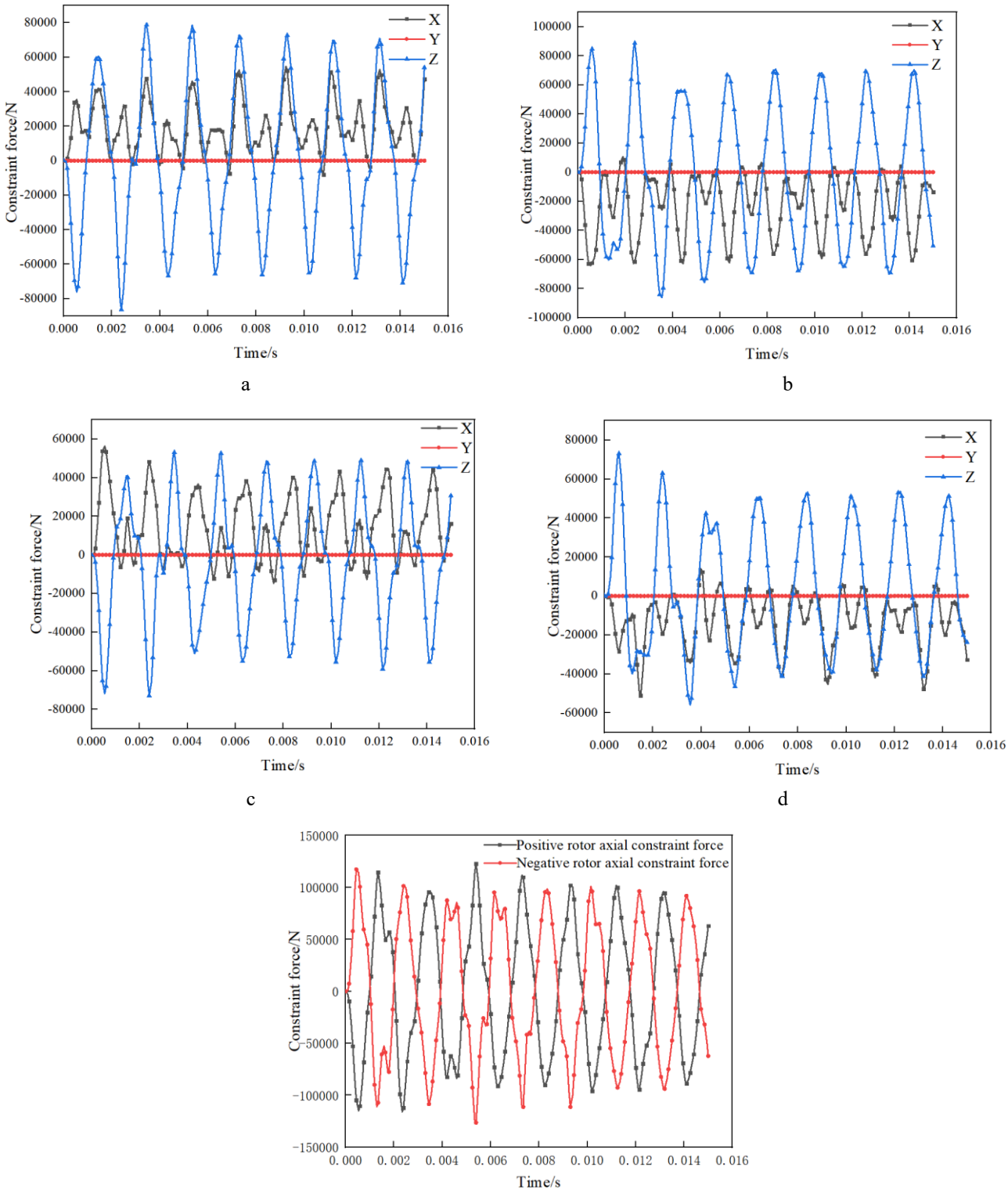

Fig. 8 Time domain binding: a – binding force at the suction end of the positive rotor, b – binding force at the suction end of the negative rotor, c – binding force at the exhaust end of the positive rote, d – binding force at the exhaust end of the negative rotor, e – axial binding force at the exhaust end of the negative and positive rotor

as friction. Considering the existence of oil lubrication in the oil injection compressor, the friction coefficient was 0.08. Finally, the curve of binding force at each constraint with time was obtained by solving, as shown in Fig. 8.

From Fig. 8, it can be seen that the binding force at the rotors bearing mounting position shows a periodic change, this is caused by the constant engagement and disengagement of the negative and positive rotors during rotation. From Figs. 8, a-d, it can be seen that the direction of the binding force on the suction and discharge ends of the positive rotor in the X direction is basically positive value, the direction of the binding force on the suction and discharge ends of the negative rotor in the X direction is basically negative value, this is because the contact force on the

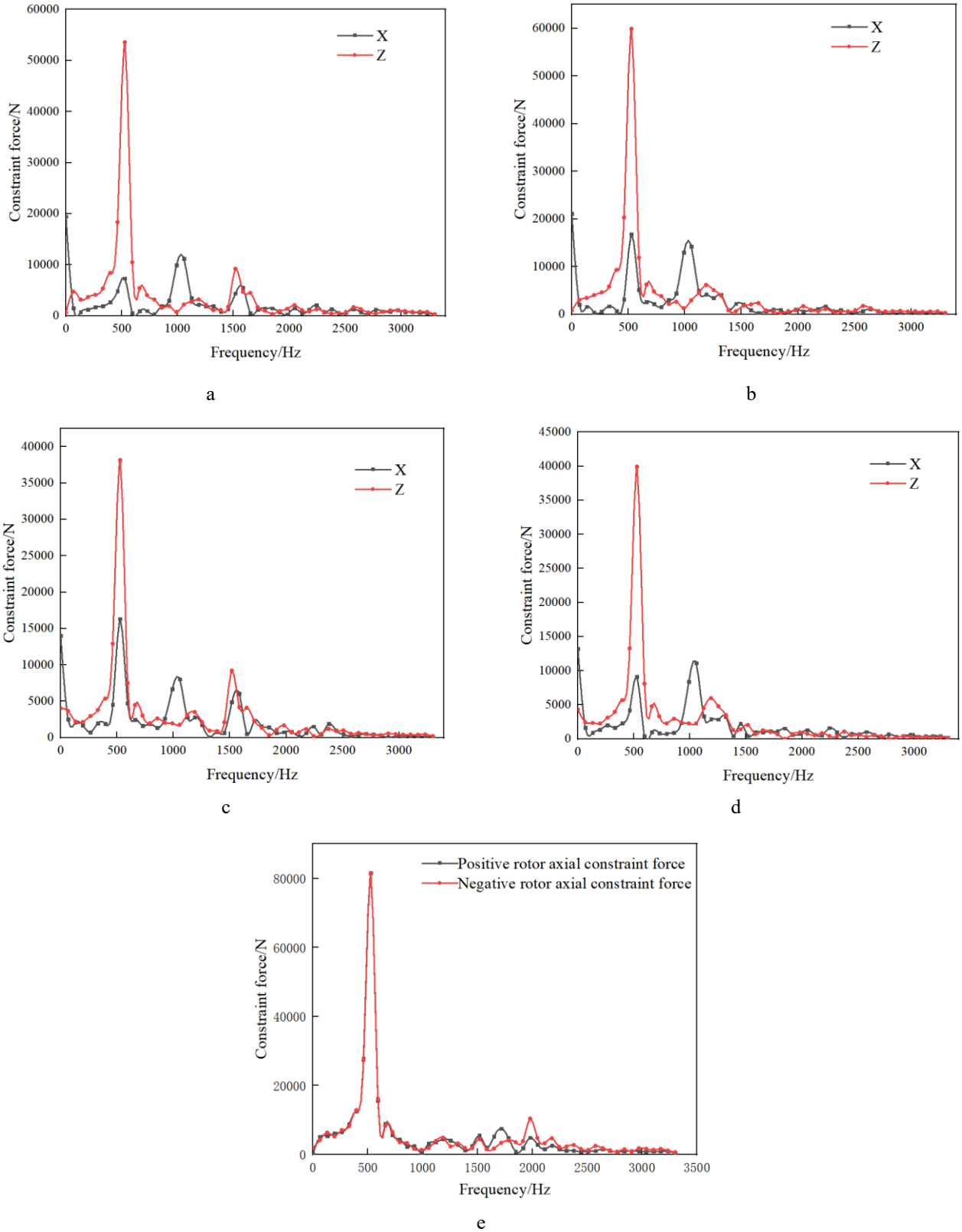

Fig. 9 Frequency domain binding: a – binding force at the suction end of the positive rotor, b – binding force at the suction end of the negative rotor, c – binding force at the exhaust end of the positive rotor, d – binding force at the suction end of the negative rotor, e – axial binding force at the exhaust end of the negative and positive rotor

negative and positive rotor is along the normal direction of the contact position, the normal direction of the contact position of the negative and positive rotor is always from the contact position to the side of its own axis, the reason for the negative direction of binding force in the X direction of the positive rotor and the positive direction of binding force in the X direction of the negative rotor is the flow field pressure on the rotor surface.

The time domain binding force is transformed by FFT to obtain the frequency domain binding force as shown in Fig. 9. As can be seen from Fig. 9, when the frequency is around 528.05 HZ, the individual binding forces are the largest, such as the radial force at the suction end of the positive rotor, the radial force at the suction end of the negative rotor, the radial force at the exhaust end of the positive rotor, the radial force at the exhaust end of the negative rotor, and the axial force at the negative and positive rotors, while the binding forces are relatively small at other frequencies.

4. Dynamics analysis of twin-screw compressor shell

The material used for the twin-screw compressor shell studied in this paper is gray cast iron HT250, and its material properties are shown in Table 2. The tetrahedral unit compressor shell is used for meshing, the cell size is set to 5 mm, the final mesh number is 522008, and the average value of cell mass and skewness are 0.83823 and 0.22764 respectively. The compressor shell mesh is divided as shown in Fig. 10.

Table 2

HT250 material parameters

Parameters	Value
Density, ρ	7280 kg/m^3
Elastic modulus, E	138 GPa
Poisson ratio, ν	0.3
Thermal expansion coefficient, α	8.2×10^{-6}/k
Thermal conductivity, λ	45 W/(m • k)

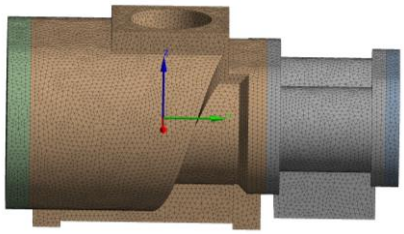

Fig. 10 Compressor case meshing

4.1. Modal analysis of twin-screw compressor shell

The excitation force generated by the rotor movement is eventually borne by the shell. To determine whether the shell resonates during the engagement of the negative and positive rotor, the inherent frequency of the compressor shell is solved by modal analysis. The compressor housing studied in this paper is bolted to the base, so for its modal analysis, only fixed constraints are applied to the base of the compressor housing to achieve limiting the degrees of freedom in six directions. According to the rotor excitation time domain force main frequency range set to solve the modal order of 6, the first six orders of the shell inherent frequency and vibration cloud diagram are shown in Fig. 11, and the inherent frequency and vibration characteristics are shown in Table 3

As can be seen from Table 3, The 1st order intrinsic frequency of the shell is 959.17 Hz and the 6th order intrinsic frequency is 2366.0 Hz, where the 2nd order intrinsic frequency is less variable than the 1st order intrinsic frequency, the fifth-order intrinsic frequency is closer to the sixth-order intrinsic frequency, however, there is a gradient increase from the 2nd order intrinsic frequency to the 5th order intrinsic frequency, and the range of variation is relatively large.

From section 2.2, the maximum rotor binding force at the maximum frequency is 528.05 Hz, then the maximum excitation force on the shell at the bearing installation position is also 528.05 Hz. By comparing with the first 6th order inherent frequency of the shell, it can be seen that the maximum excitation force on the shell is far from the first 6th order inherent frequency, so the compressor shell will not resonate with the negative rotor and the positive rotor during their engagement. Therefore, the compressor shell does not resonate with the negative and positive rotor during their engagement.

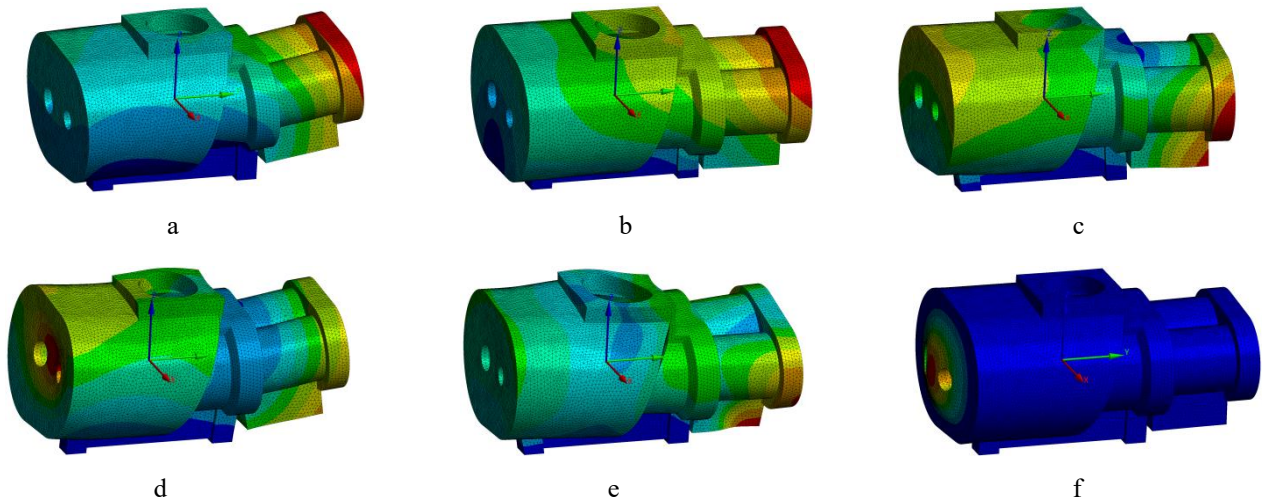

a b c

d e f

Fig. 11 Shell first sixth modes: a – first natural frequency 959.17 Hz, b – second natural frequency 1027.7 Hz, c – third natural frequency 1346.3 Hz, d – fourth natural frequency 1692.9 Hz, e – fifth natural frequency 2233 Hz, f – sixth natural frequency 2366 Hz

Table 3

Natural modes and mode shapes of the shell

Number of steps	Inherent frequency, Hz	Inherent vibration pattern
1	959.17	Bending vibration of the exhaust end and right end cap in the Z direction
2	1027.7	The shell vibrates around the Y-direction twist
3	1346.3	Shell bending vibration in X direction
4	1692.9	The left end cap is depressed and the rest of it is bent in the Z-direction
5	2233.0	The suction end is twisted, the exhaust end is bent in the X direction and twisted around the Y direction
6	2366.0	The left end cap is repeatedly recessed and raised along the Y direction

4.2. Transient dynamics analysis of twin-screw compressor shells

For the transient dynamics analysis of the compressor shell, the mesh division and constraint settings are the same as in the previous section. The pressure field obtained from the flow field analysis is applied to the inner wall surface of the shell, and the rotor binding force reaction is used as one of the compressor shell vibration excitation sources and applied to the bearing mounting position in the shell, and the load is applied as in Fig. 12. The analysis time is set to 0.015 s and the time step is 200 steps to solve the dynamic response of the compressor housing during one week of rotation of the positive rotor.

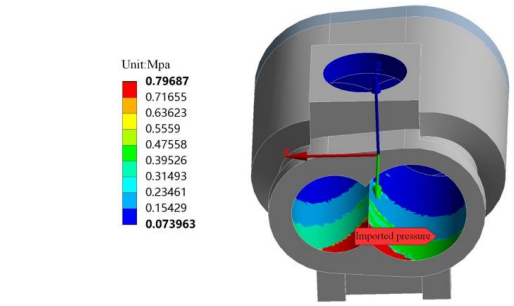

a

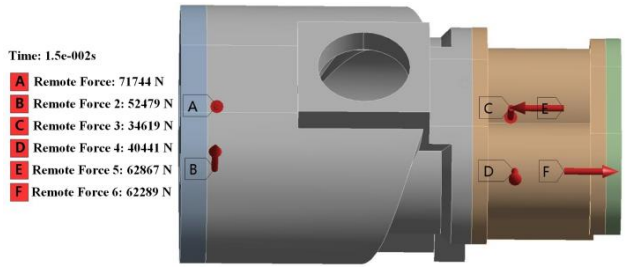

b

Fig. 12 Excitation force of the compressor shell: a – pressure load, b – rotor binding reaction force

In the vibration response analysis of the compressor shell, the physical quantity of vibration displacement is used to measure the magnitude of shell vibration. The vibration displacement is a vector quantity, with positive values indicating the same direction as the positive direction of the corresponding axis, and negative values indicating the opposite direction of the positive direction of the corresponding axis. The compressor shell vibration displacement maximum curve and deformation cloud diagram are shown in Fig. 13 and Fig. 14.

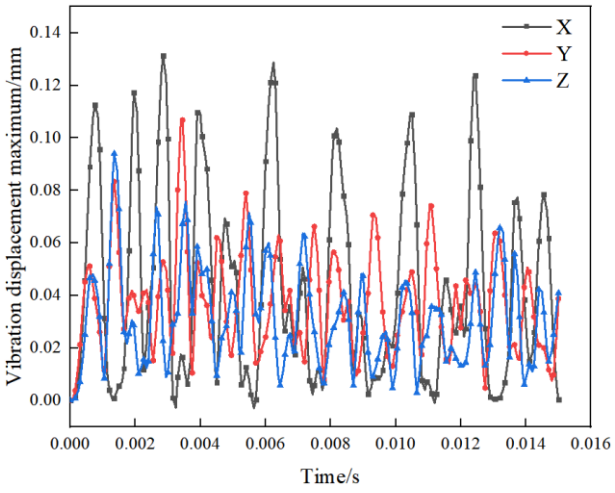

a

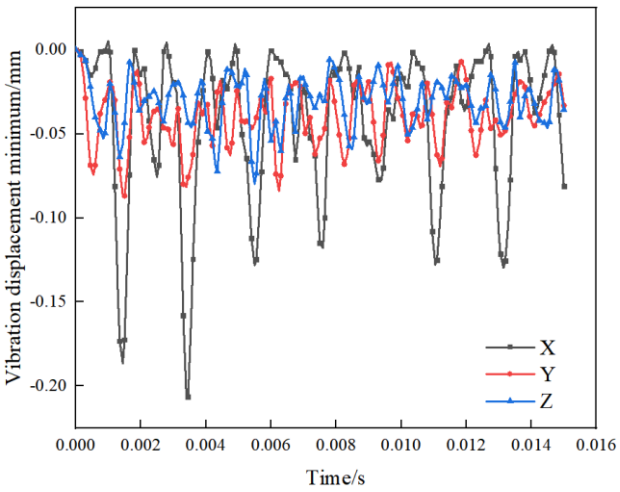

b

Fig. 13 Shell vibration displacement: a – vibration displacement maximum, b – vibration displacement minimum

Fig. 13, a and Fig. 13, b show the vibration displacement maximum and minimum curves of the twin-screw compressor shell in the X, Y and Z directions, respectively, as can be seen from the figure, the maximum value of vibration displacement in three directions appears in X direction, the value is 0.1312 mm, and the time of maximum value is 0.00285 s; the minimum value of vibration displacement in three directions also appears in X direction, the value is -0.2063 mm, and the time of minimum value is

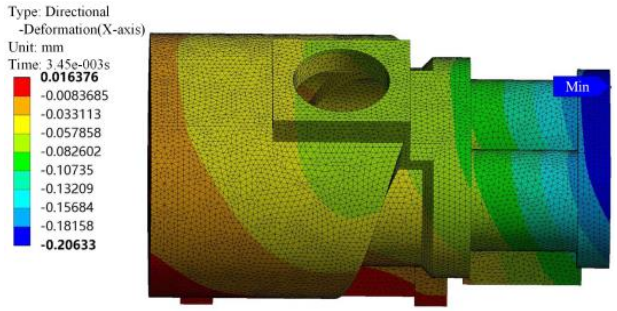

Fig. 14 Displacement cloud image

0.00345 s. Comparing the extreme value of vibration displacement for the whole period of time, the maximum value of vibration displacement in X direction is generally larger than the maximum value of vibration displacement in Y direction, and the maximum value of vibration displacement in Y direction is generally larger than the maximum value of vibration displacement in Z direction; while the minimum value of displacement in Z direction is generally larger than the minimum value of displacement in Y direction, and the minimum value of displacement in Y direction is generally larger than the minimum value of vibration displacement in X direction. It can be seen that the twin-screw compressor shell has the largest absolute value of vibration displacement in the X direction and the smallest absolute value of vibration displacement in the Z direction. Fig. 14 shows the displacement cloud map at the maximum moment of the absolute value of vibration displacement in the X direction at 0.00345 s, it can be seen from Fig. 14 that the location where the maximum value of the absolute value of the vibration displacement occurs in the X direction is the right end cap in the shell.

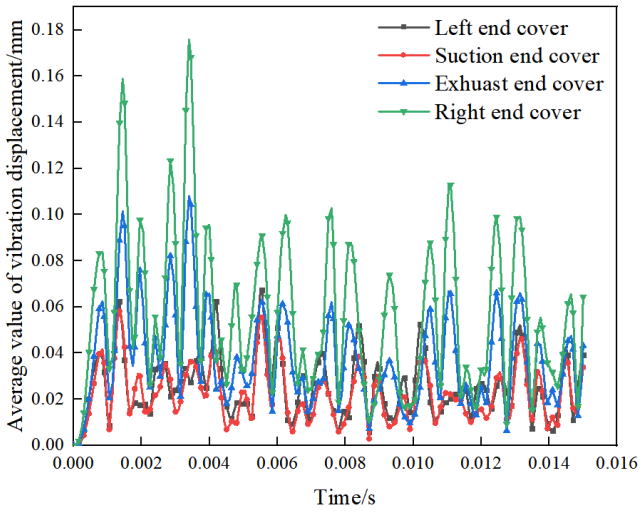

Fig. 15 Average value of vibration displacement of each part of the shell

In order to compare the surface vibration response of the compressor shell more intuitively and provide reference for subsequent shell damping design, the compressor shell was divided into four parts, namely, the left end cover, the suction end, the exhaust end and the right end cover, and the average value of vibration displacement of the four parts was extracted. The average vibration displacement curves for the four parts of the twin-screw compressor shell are shown in Fig. 15. As shown in Fig. 15, the maximum average vibration displacement of the left end cover, suction end, exhaust end and right end cover of the compressor shell is 0.06721 mm, 0.05770 mm, 0.10435 mm, and 0.16816 mm in order. From the distribution position of the curve, it can be seen that within the solution period, the four parts are sorted from largest to smallest according to the average value of vibration displacement, and the four parts are sorted as right end cover, exhaust end, left end cover and suction end. That is, the contribution of the right end cover to the vibration displacement of the compressor shell is relatively large, and the contribution of the suction end to the vibration displacement of the compressor shell is relatively small.

5. Conclusions

In this paper, based on the fluid-structure coupling method, the flow field distribution of the twin-screw compressor is first solved, then the rotor binding force is solved by applying the flow field pressure to the rotor surface, and the case resonance is determined by comparing the frequency domain of the constraint force with the compressor shell inherent frequency, finally the vibration response analysis of the compressor shell was carried out, and the following conclusions were drawn:

1. The flow field force in the compressor flow field is increasing as it gets closer to the discharge port, but the change in flow field force from the suction end to the exhaust end is non-linear, and the closer it is to the discharge port, the larger the pressure jump is.

2. The binding force on the negative and positive rotors at the bearing mounting position varies periodically with time, and the peak of the binding force at each location is 528.05 Hz through frequency domain analysis, which is far away from the shell inherent frequency and will not cause shell resonance during the negative and positive rotor meshing process.

3. Under the action of flow field force and rotor restraint reaction force, the absolute value of vibration displacement of the compressor shell in the X direction is the largest, and the largest position appears in the right end cover of the shell; and the contribution of each part of the shell to the vibration displacement from the largest to the smallest is the right end cover, exhaust end, left end cover and suction end.

Through the research of this paper, it can be seen that in the design of the compressor, the frequency of the excitation force on the rotor under the working speed and the intrinsic frequency of the shell should be considered comprehensively to avoid the resonance phenomenon during the working process; for the vibration displacement of the different parts of the shell, it can be improved by adding reinforcing bars, optimizing the wall thickness of the shell, and increasing the vibration-damping pads and other ways.

Acknowledgments

This work was supported by the Science Technology Department Key Project of Shaanxi Province (No: 2017ZDXM-GY-138).

References

1. **Xue, H. Q.; Zhang, G. J.; Hu, L. F**. et al. 2021. Calculation and Analysis of Radiation Noise Characteristics of a Type of Marine Air Compressors, Noise and Vibration Control 41(04): 115-121. https://doi.org/10.3969/j.issn.1006-1355.2021.04.018.
2. **Huang, Z. Q.; Yang, R. S.; Li, G.** et al. 2022. Vibration analysis and test study of large reciprocating compressor host, Chinese Journal of Engineering Design 29(04): 465-473. https://doi.org/10.3785/j.issn.1006-754X.2022.00.051.
3. **Bakhtiaryfard, L.; Chen, S. X.; Wu, Y**. **R.** et al. 2018. Vibration Analysis of Twin-Screw Compressors Under Partial Load Design: A Case Study, International Compressor Engineering Conference, Inc. 2018: 189-198. https://docs.lib.purdue.edu/icec/2541/.
4. **Li, C.; Wang, H. H.; Zhang, X. D**. et al. 2021. Study on the dynamic characteristics of scroll compressor rotor system considering the influence of clearance, Fluid Machinery 49(01): 43-50. https://doi.org/10.3969/j.issn.1005-0329.2021.01.007.
5. **Jiang, S. J.; Zhang, Y. H.; Shi, Y. F.** et al. 2020. Experimental Research and Simulation Analysis of Impeller Vibration Characteristics of Centrifugal Compressor, Machinery Design and Manufacture (05): 19-22. https://doi.org/10.3969/j.issn.1001-3997.2020.05.005.
6. **Li, S. X.; Kang, Y. X.; Pan, W. L.** et al. 2019. Analysis and Optimization of Pipeline Vibration of Reciprocating Compressors, Fluid Machinery 47(02): 58-64. https://doi.org/10.3969/j.issn.1005-0329.2019.02.011.
7. **Wang, C.; Wang, Z.; Yan, W.** et al. 2021. Study on Characteristics of the Vibration and Noise of High-Power Scroll Compressor, Shock and Vibration (2021): 1-17. https://doi.org/10.1155/2021/5953133.
8. **Liu, L. B.; Wu, T.** 2020. Experimental Study on the Vibration Contribution of Scroll Compressor Components, Fluid Machinery 48(9): 6-11, 64. https://doi.org/10.3969/j.issn.1005-0329.2020.09.002.
9. **Xu, C.; Zhou, H.; Mao, Y.** 2020. Analysis of vibration and noise induced by unsteady flow inside a centrifugal compressor, Aerospace Science and Technology 107: 106286. https://doi.org/10.1016/j.ast.2020.106286.
10. **Yang, F.; Lu, J. W.; Ren, Y. K.** et al. 2022, Dynamic response analysis of air conditioning pipeline considering fluid-structure interaction, Journal of Hefei University of Technology (Natural Science) 45(5): 597-601, 609. https://doi.org/10.3969/j.issn.1003-5060.2022.05.004.
11. **Li, T. L.; Wang, J. L.; Lei, S.** et al. 2020. Numerical simulation method of rotor structure characteristics of twin-screw compressor rotor, Journal of Mechanical & Electrical Engineering 37(10): 1192-1197, 1209. https://doi.org/10.3969/j.issn.1001-4551.2020.10.011.
12. **He, Y. Y.; Gao, W. L.; Liang, Z. H.** 2020. Study on vibration characteristics of shell structure of twin-screw air compressor, Journal of Shaanxi University of Technology (Natural Science Edition) 36(04): 1-6. https://doi.org/10.3969/j.issn.1673-2944.2020.04.001.
13. **Zeng, R.; Hou, L.; You, Y. X.** et al. 2019. Transient Dynamic Analysis of Cylinder of High-Pressure Simulator, Machinery Design & Manufacture (S1): 99-103. https://doi.org/10.3969/j.issn.1001-3997.2019.z1.024.

Y. He, W. Zhang, X. He, K. Wang, J. Wang, Y. Zhao

VIBRATION CHARACTERISTICS ANALYSIS OF TWIN-SCREW COMPRESSOR SHELL BASED ON THE FLUID-SOLID COUPLING METHOD

S u m m a r y

Under the action of the flow field force and the constraint reaction force of the negative rotor and the positive rotor, the twin screw compressor shell will produce vibration, which will affect the life of the parts and produce noise. The rotors restraint reaction force is calculated by fluid-structure coupling method. The shell inherent frequency is solved by modal analysis, and the shell resonance is analyzed during the rotors meshing process. On this basis, the flow field force and rotor constraint reaction force are used as the compressor shell vibration excitation sources, and the vibration response of the compressor shell under the action of excitation force is studied. The research results can provide some reference for the optimized design of compressor shell structure.

Keywords: twin-screw compressor, fluid-structure coupling, rotor engaging, excitation source, vibration.

Received January 11, 2023
Accepted April 15, 2024